In: *Process Tomography -1995*, by Beck, M.S. et al (Eds.), Proceedings of the 4th Workshop of the European Concerted Action on Process Tomography, Bergen, 6-8 April, 1995, p401-410.

Regularised Image Reconstruction of Noisy Electrical Resistance Tomography Data

Binley, A.[1], Ramirez, A.[2] and Daily, W.[2]

[1] *C R E S, Institute of Environmental and Biological Sciences, Lancaster University, Lancaster, LA1 4YQ, U.K.*

[2] *Lawrence Livermore National Laboratory, Livermore, CA 94550, U.S.A.*

ABSTRACT: Electrical resistance tomography may be used to obtain qualitative or quantitative information about the spatial distribution of resistivity within a body of interest. Whereas image reconstruction techniques for the former such as back projection methods are often insensitive to data errors, reconstruction of quantitative images may be highly sensitive. In many cases, lack of information about errors in the data may lead to poor images or failure to obtain a solution to the inverse model. Simple methods may be utilised to characterise data error, which are discussed here. We demonstrate the role of data error on reconstruction, focusing on a regularised inverse method which has been shown to be robust for many real applications.

KEYWORDS: *Electrical Resistance Tomography, Data Error, Image Reconstruction, Inverse Methods*

1. INTRODUCTION

The primary objective of electrical resistance tomography (ERT) is to gain some knowledge of the spatial variation of electrical resistivities within some body, given measurements of resistance taken within the body. This is shown schematically in figure 1 for the case where the body is a circular vessel.

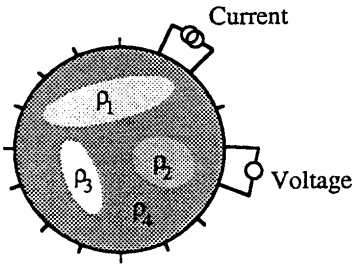

Fig. 1: Electrical resistance tomography

Adopting a 4 electrode approach the potential difference between different pairs of electrodes combined with knowledge of the injected current allows us to build up a pattern of transfer resistances (measured potential difference for a unit applied current). We may then repeat this procedure for combinations of the simple four electrode measurement. Given a set of such measurements we are able to determine the internal resistivity distribution within the body under examination using some appropriate image reconstruction technique.

2. CHARACTERISATION OF DATA ERROR

Electrode measurements will be subject to a variety of error sources. Poor electrode contact may result in systematic errors associated with particular electrodes, more random errors may arise due to the measurement device and, in addition, sporadic errors may occur due to non-deterministic external effects. There is then a need to characterise the measurements in terms of likely error. Two simple ways of achieving this goal involve determination of repeatability and reciprocity of the measurements.

Repeatability is obvious, one repeats measurements for each four electrode configuration, making sure that temporal affects, such as polarisation, are not induced by the procedure. A second method of characterisation involves making use of the reciprocal behaviour of four electrode measurements. The current source (C+) and sink (C-) electrode may be reversed which should result in identical readings with reversed polarity. Similarly the positive potential (P+) and negative potential (P-) electrodes may be switched to the same effect.

In addition use may be made of the reciprocity effect by which current and potential electrodes may be exchanged. A comparison of the two will reveal inconsistency with the reciprocal behaviour expected under ideal conditions. In total eight readings should give identical magnitude of the measured transfer resistance.

We may consider a simple error model in which the data variance σ^2 increases with the square of the transfer resistance R with slope ψ for large resistances and a minimum data variance of ϕ^2 is observed, that is:

$$\sigma^2 = \phi^2 + \psi R^2 \tag{1}$$

Our error model (and inversion that follows) will assume that random errors possess a zero mean and are normally distributed. Plots of repeatability and reciprocal error may reveal how appropriate these assumptions are. For example, consider the reciprocal error plot shown in figure 2 for a 15cm diameter saline filled phantom using a combination of 'nearest neighbour' and 'opposite' measurement protocols. For the former current is injected between an adjacent pair of electrodes and the potential difference is measured between all other adjacent electrodes. For the latter

current is driven between diametrically opposite electrodes and potential difference measured between adjacent electrodes. All measurements appear to be scattered symmetrically about a zero error and follow well the error model above.

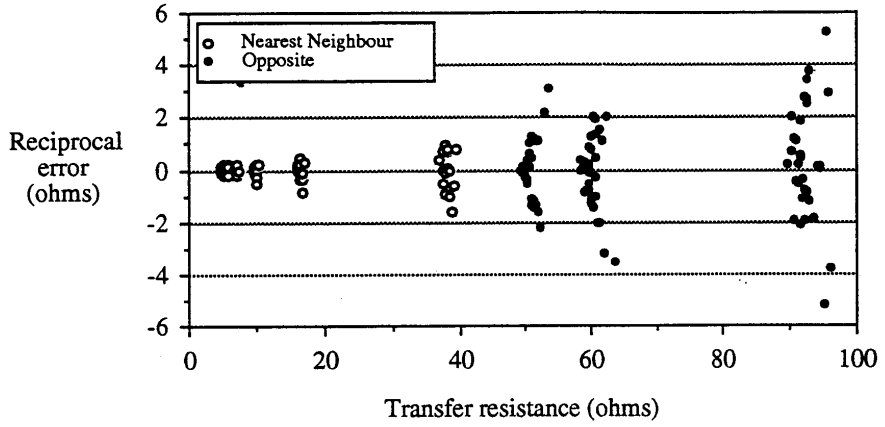

Fig. 2: Reciprocal error using nearest neighbour and opposite measurements for 15cm diameter saline phantom

Plots such as that in figure 2 are useful in determining spurious measurements as any readings which do not follow the simple relationship above which may be rejected (or remeasured) prior to any inversion of the data.

3. REGULARISED IMAGE RECONSTRUCTION

Given some assessment of error in our measurements we are now able to consider the inversion of the data to produce a map of the distribution of resistivities within the body of interest.

The model of a source free conducting inhomogeneous body Ω, with resistivity distribution $\rho(x, y)$, into which steady-state current is injected and the corresponding transfer resistance R is measured, is governed by the following generalised Maxwell equation:

$$\nabla . \rho^{-1} \nabla v = 0 \tag{2}$$

Equation (2) is a second order partial differential in voltage v which, for inhomogeneous current distributions, can only be solved numerically. Various schemes are available for the forward solution, the finite element method often being preferred due to its superior geometrical properties. By employing the finite element method,

equation (2) is reduced to a set of linear simultaneous equations describing the potential distribution within the domain of interest. Computation of voltage at the electrode locations may then be used to derive the transfer resistance for a given four electrode measurement.

The formal inverse problem attempts to determine the M resistivities $\rho_j \quad j = 1, 2, ...M$ (which we will refer to as vector of parameters $\mathbf{m}$) from a finite number of N resistance measurements $R_i \quad i = 1, 2, ...N$ and boundary conditions. We may use the finite elements to define the parameter boundaries, alternatively we may solve the forward solution on a finely discretised mesh and group or block elements to define parameter regions.

If we define $\mathbf{D}$ as the vector of measured transfer resistances and $\mathbf{F(m)}$ as the corresponding forward solution transfer resistances using parameters $\mathbf{m}$ then we may define a weighted least squares objective function as:

$$\chi^2 = (\mathbf{D} - \mathbf{F(m)})^T \mathbf{W}^T \mathbf{W} (\mathbf{D} - \mathbf{F(m)}) \tag{3}$$

Where $\mathbf{W}$ is a weight matrix which quantifies the uncertainty in our data $\mathbf{D}$. If there is a high level of uncertainty in a particular measurement then it should be weighted less than the other data. If we neglect off diagonal terms in $\mathbf{W}$, that is treat the errors as uncorrelated, then $\mathbf{W}$ is simplified using the data standard deviations ($\sigma_i, \quad i = 1, 2, 3, ..., N$), that is:

$$W_i = \frac{1}{\sigma_i}$$

Minimisation of the objective function in (3) results in the well known Marquardt method (Marquardt[1]). Note that the objective function in (3) is simply concerned with minimisation of the data misfit. This may at first appear to be the only concern for image reconstruction, however, in many cases we are able to use additional information to assist in the inverse solution. The Marquardt method will often produce extremely *rough* images by forcing the data misfit to its minimum and yet there may be some knowledge that a *smooth* image is more realistic. For example, in the case of geological systems one may expect abrupt changes in certain systems but often there will be some degree of spatial correlation of the property of interest. Pixel values will be, in some way, related to adjacent pixel values. In some cases the correlation may be low, nevertheless this qualitative *a priori* information should be used within the reconstruction.

Fortunately, to constrain image reconstruction so that smoother models are preferred is relatively easy. Tikhonov first devised a scheme, referred to as regularisation (see for example, Tikhonov and Arsenin[2]), which makes the inverse solution more well-posed by forcing some dependence between the parameters values. This approach

may also be justified on the grounds of *a priori* information about such dependence, with an added benefit of a less ill-posed solution. A number of geophysicists have realised this (see for example, Constable et al.[3]; Sasaki[4]) and employed regularisation for subsurface imaging with great success.

To employ regularisation the objective function may be rewritten as:

$$(\mathbf{D} - \mathbf{F}(\mathbf{m}))^T \mathbf{W}^T \mathbf{W} (\mathbf{D} - \mathbf{F}(\mathbf{m})) + \alpha \mathbf{m}^T \mathbf{R} \mathbf{m} \tag{4}$$

Where $\mathbf{R}$ is a square *roughness matrix* which is fixed and controls the scale of parameter dependence throughout the image. In (4) α is a scaling parameter which may be fixed or allowed to vary throughout the inverse solution.

The roughness matrix $\mathbf{R}$ may take various forms but will usually consist of positive and negative integers in a banded structure. A first or second derivative difference operator may be suitable for most applications. Sasaki[4] presents a roughness matrix for a two dimensional quadrilateral finite element meshes. For the case considered here the region is discretised into triangular blocks (finite elements). A roughness matrix for this mesh may be formed in a similar manner to that of Sasaki[4], in this case as a zero matrix with, on each row, unity for the three triangles adjacent to the triangle corresponding to that row and -3 on the diagonal. Other schemes are possible.

Minimising the objective function in (4) we may write the following iterative equations:

$$\begin{aligned} [\mathbf{J}^T \mathbf{W}^T \mathbf{W} \mathbf{J} + \alpha \mathbf{R}] \Delta \mathbf{m} &= \mathbf{J}^T \mathbf{W}^T \mathbf{W} (\mathbf{D} - \mathbf{F}(\mathbf{m})) - \alpha \mathbf{R} \mathbf{m} \\ \mathbf{m}_{i+1} &= \mathbf{m}_i + \Delta \mathbf{m} \end{aligned} \tag{5}$$

where $\mathbf{J}$ is the Jacobian given by:

$$J_{i,j} = \frac{\partial F_i(\mathbf{m})}{\partial m_j},$$

$\mathbf{F}(\mathbf{m})$ is evaluated at $\mathbf{m}_i$.

It can easily be seen that as α approaches zero the scheme approaches that of the basic weighted least squares method as one would expect from the objective function in (4).

In its simplest form a constant α may be selected (see for example, Sasaki[4]; Sasaki[5]). Constable et al.[3] and deGroot-Hedlin and Constable[6] have argued

that iteratively selecting α will lead to a more desirable solution, particularly as one is often unable to select the smoothing parameter *a priori*. For the examples presented here α is determined at each iteration in such a way that the data misfit is minimised at each step. In order to do this several sub iterations are required at each iteration of the main scheme, although the computational effort for this need not be excessive (Constable et al.[3]).

4. DATA ERROR AND INVERSION

Given the solution scheme we now draw attention to role of data error on the reconstruction. Figure 3a shows a synthetic model with a 1000 Ωcm anomaly in a 100 Ωcm region which was used to compute a dataset for inversion. The measurement scheme used was a combination of 'nearest neighbour' and 'opposite' data, as outlined in section 2. Using noise-free data, the regularised inverse solution produces the model in figure 3b. In order to minimise numerical discretisation errors the forward solution component of the image reconstruction was based on a finite element mesh of 312 roughly equilateral triangular finite elements. For the inverse solution the mesh was then parametrised into 104 triangular blocks, each based on 3 of the elements used for the forward solution.

Adding 5% Gaussian noise to the data prior to inversion, that is, setting ψ in (1) to 0.05, the data were inverted using a correct form of the weight matrix in (4). That is, the exact nature of the error distribution was known prior to inversion. The resulting model in shown in figure 4a. Failure to achieve the correct magnitude of the resistive anomaly is seen due to the noise level of the data, nevertheless, location of the feature is precise. In contrast the same noisy data were inverted without any prior knowledge of data error, that is, all measurements were equally weighted. Figure 4b shows the result of this inversion, in which incorrect features are created as artifacts of the noise.

It is clear from this example that the form of any data error is essential for correct reconstruction. Determination of data error magnitude may be evaluated using repeatability and/or reciprocity checks as outlined earlier. These estimates may be assessed following image reconstruction using the final normalised model error:

$$\epsilon_i = \frac{D_i - F(\mathbf{m})}{\sigma_i} \qquad i = 1, 2, 3, ..., N$$

Where $F(\mathbf{m})$ is evaluated at the final model $\mathbf{m}$.

If the assumptions of zero mean uncorrelated error are correct then the values of ϵ should lie roughly between -3 and +3 and show no distinct trends. To illustrate this figure 5a shows the normalised error, computed as above, for the model in figure

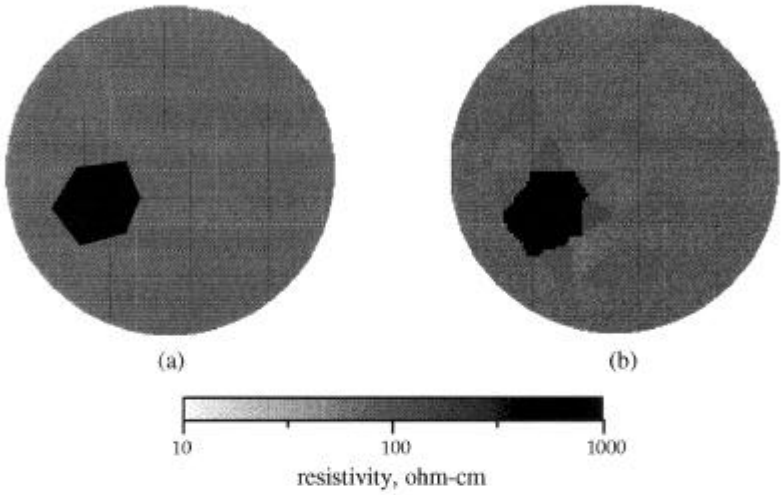

Fig. 3: Image reconstruction from noise free data.
(a) True model (b) Final image

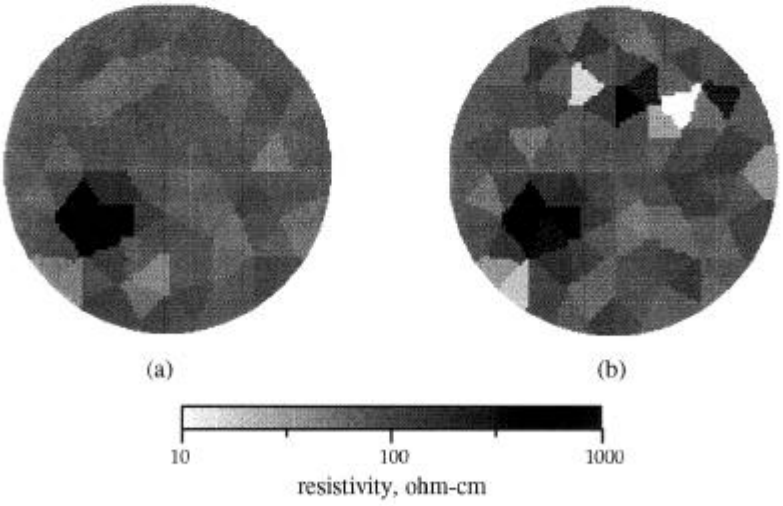

Fig. 4 : Image reconstruction from noisy data.
(a) Weighted with true error (b) unweighted

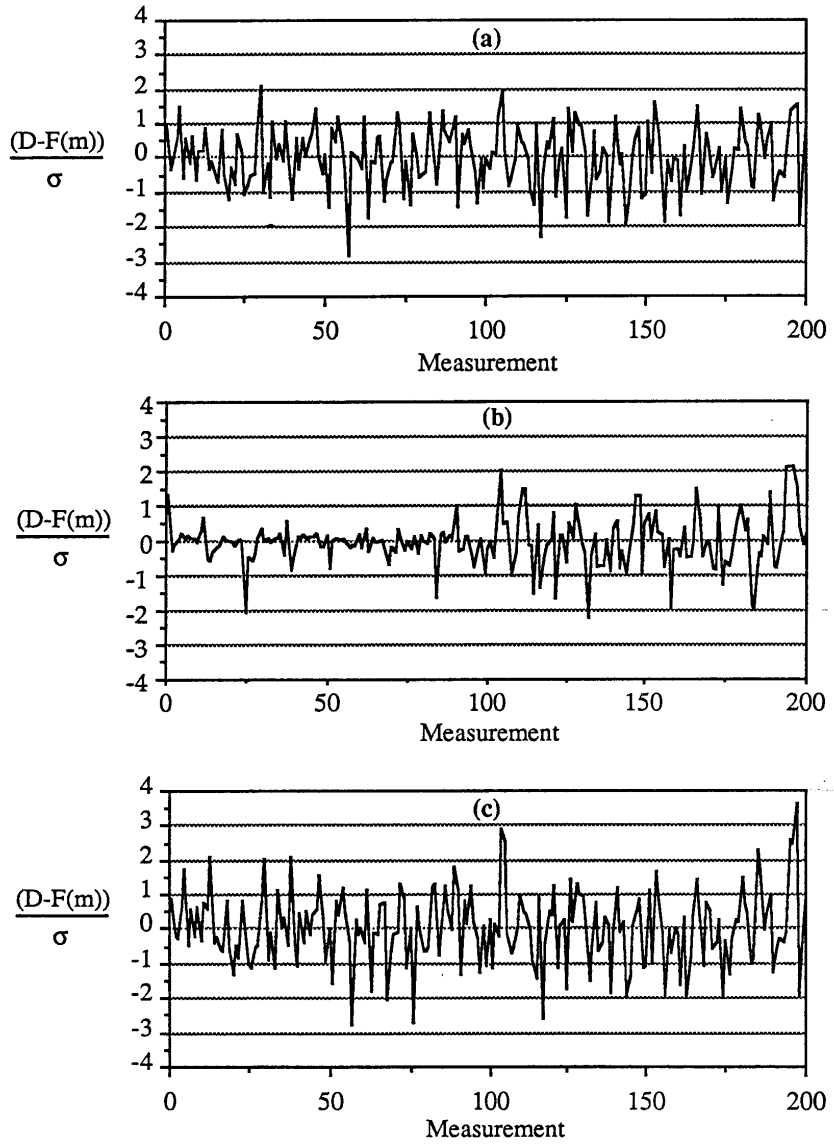

Fig. 5: Final model residual error for model in figure 3a.
(a) 5% noise added to data and inverted as figure 4a, (b) 5% noise added and inverted as figure 4b, (c) 5% noise added with 10% noise at electrode 1.

4a, that is, reconstruction with the correct error assessment. In contrast, figure 5b shows the normalised error for the model of figure 4b produced with incorrect error weighting. The first 104 measurements in this latter case show a normalised error which is far too low and significantly different from the remaining 96 measurements. These first 104 measurement correspond to nearest neighbour measurements, which have in effect been weighted too little in this case by the use of incorrect uniform weighting for the composite measurement scheme.

The plot of normalised error may also be used to reveal more subtle inconsistencies. For example, figure 5c shows the final model errors for the reconstruction of data generated using again the starting model in figure 3a with 5% Gaussian noise added to the data. This case differs from that in figure 5a by increasing the error to 10% for all measurements that used the first electrode for any potential reading. This will then mimic a case possibly where poor electrode contact is realised at one (or more) location (a common occurrence when dealing with porous media or similar materials). One can now observe that the normalised errors for the final model for this case generally follow the ideal pattern, however, a small number are noticeably too high.

5. CONCLUSIONS

Errors in electrical resistance tomography data is unavoidable. The magnitude may be minimised by appropriate instrument design and suitable electrode connections, however, if quantitative images are required from the data, an assessment of the degree of data error can vastly improve model evaluation. Regularised inverse models provide robust tools for image reconstruction but like all non-linear inverse methods are sensitive to noise levels in the data. Avoidance of fitting noise rather than data is obviously necessary and yet this significant component of tomographic imaging is often neglected. For resistance imaging use may be made of repeatability and reciprocity checks to provide a useful guideline of the error levels and indicate any clear outliners in the measurements. The results of the final inverse model may also be used to confirm initial error estimates or reveal inconsistencies with the model assumptions. For models changing temporally, noise levels may change. Normalised errors plots will reveal these changes and any autocorrelation in the errors with little computational effort.

ACKNOWLEDGEMENTS

This work has been supported by funding from the Natural Environment Research Council, Grant number GR3/9087. Thanks to Siobhan Henry-Poulter and Ben Shaw for data acquisition.

REFERENCES

[1] Marquardt, D.W., An algorithm for least-squares estimation of non-linear parameters, *J. S.I.A.M.*, Vol. 11, p431-441, 1963.

[2] Tikhonov, A.N. and V.Y. Arsenin, *Solution of ill-posed problems*, Wiley, 1977.

[3] Constable, S.C., R.L. Parker and C.G. Constable, Occam's inversion: A practical algorithm for generating smooth models from electromagnetic sounding data, *Geophysics*, Vol. 52(3), p289-300, 1987.

[4] Sasaki, Y., Two-dimensional joint inversion of magnetotelluric and dipole-dipole resistivity data, *Geophysics*, Vol. 54, p254-262, 1989.

[5] Sasaki, Y, Resolution of resistivity tomography inferred from numerical simulation, *Geophysical Prospecting*, Vol. 40, p453-463, 1992.

[6] deGroot-Hedlin, C. and S. Contable, Occam's inversion to generate smooth, two-dimensional models from magnetotelluric data, *Geophysics*, Vol. 55(12), p1613-1624, 1990.